




# Optimization of process and properties of biochar from cabbage waste by response surface methodology

Snigdhendubala Pradhan<sup>1</sup> · Muhammad Shahbaz<sup>1</sup> · Ali Abdelaal<sup>1</sup> · Tareq Al-Ansari<sup>1,2</sup> · Hamish R. Mackey<sup>1</sup>  · Gordon McKay<sup>1</sup>

Received: 12 June 2020 / Revised: 14 October 2020 / Accepted: 16 October 2020 / Published online: 9 November 2020  
© Springer-Verlag GmbH Germany, part of Springer Nature 2020

## Abstract

The properties of biochar produced by pyrolysis are strongly influenced by various factors such as feedstock. Cabbage makes up around 6.5% of global vegetable production with around 30% wasted from the farm to plate, making it a considerable and widely available biochar feedstock. This study investigates the optimization of three design factors, namely, pyrolysis temperature, feed particle size, and quantity of waste cabbage biomass to produce biochar. Feed particle size was selected due to its relevance to solar or other drying pretreatment, necessary for moisture reduction. To evaluate the influence of these parameters and find their optimum conditions, response surface methodology (RSM) with a central composite design of experiments was used. Optimum response for cabbage biochar was observed at lower temperature (360 °C) with particle size of 0.90 mm and a relatively low quantity, though this latter parameter had minimal influence on most response parameters. Temperature was the most influential parameter on all response variables, although particle size was important for nitrogen content, cation exchange capacity (CEC), and electrical conductivity. Biochar produced at an optimum pyrolysis temperature of 360 °C and nearest practical size of 1 mm was tested with *Ipomoea purpurea* in sandy soil. Two percent biochar loading provided an increase in water retention from 6.5% in the control to 10% in the biochar amended soil ( $p = 0.016$ ). Increases were also observed in plant height and leaf production but were not statistically significant at  $\alpha = 0.05$ .

**Keywords** Biochar · Soil fertility · Optimization · Response surface methodology · Food waste valorization · Pyrolysis

## 1 Introduction

Biochar is a carbon rich soil amendment material that has been gaining increased attention and use due to its potential applications to mitigate soil degradation, food insecurity, water pollution from agricultural sources, and global climate change [1]. Biochar is not only a soil amendment agent but also can act as an adsorbent to remove organic and inorganic

pollutants [2]. Various types of biomass such as wood materials, agricultural residues, dairy manure, sewage, and sludge have been used to produce biochars under different thermal processes and conditions. Agricultural products such as fruits and vegetables have a crucial role in human life, and the demand for food commodities has increased significantly due to growing world population [3]. Through natural processing losses and often poor handling methods, large quantities of vegetable wastes can arise. From a survey, it was estimated that the total value of fruit and vegetable wastes generated at the retail and consumer levels in the USA was \$42.8 billion in 2008 [4]. FAO in [5] revealed that during processing, packaging, distribution, and consumption of fruits and vegetables in the developed parts of China, India, the Philippines, and the USA, approximately 55 million metric tons (MMT) of wastes are produced per day. Laufenberg in [6] estimated a minimum of 70.2 MMT of vegetable wastes were generated from processing of 865.8 MMT of vegetables. Cabbage and other brassicas are one significant vegetable produced globally, with worldwide production estimated at 71.4 MMT in 2017,

**Electronic supplementary material** The online version of this article (<https://doi.org/10.1007/s13399-020-01101-5>) contains supplementary material, which is available to authorized users.

✉ Hamish R. Mackey  
hmackey@hbku.edu.qa

<sup>1</sup> Division of Sustainable Development, College of Science and Engineering, Hamad Bin Khalifa University, Doha, Qatar

<sup>2</sup> Division of Management and Decision Sciences, College of Science and Engineering, Hamad Bin Khalifa University, Doha, Qatar

making up around 6.5% of total vegetable production [7]. On an average, 30 to 50% of cabbage waste is generated during its cutting in farms, transportation, selling in markets, and further processing in kitchens before cooking [8]. Cabbage and cauliflower wastes decompose readily and thus these create greenhouse gas emissions, unpleasant odors, and flies in the open environment. One approach to obtain value from cabbage waste is to recycle the cabbage biomass in the form of low-cost soil amendment biochars to improve soil fertility and plant growth.

Various authors have reported that the biochar yield is usually high when produced from the feedstock materials rich in lignin/cellulose content [9]. Cabbage is relatively cellulose rich, with the stalks containing around 37 % cellulose on dry weight basis [10]. Typically this is seen as a disadvantage compared to lignin rich agricultural residues, since cellulose has a lower yield than lignin rich feedstocks [9]. However, cellulose also leads to reasonable yield, and higher volatile (biofuel gas) production, which can be simultaneously produced. Moreover, pyrolyzed cellulose has lower hydrogen to carbon ratio (H/C) ratio, indicative of high stability [11]. Cellulose is likely to have greater cation exchange capacity than lignin due to its higher O/C ratio [11]. Cabbage also has a relatively high trace mineral content, particularly with respect to Mn. In our recent work exploring biochar characteristics from a number of vegetable wastes, cabbage showed promising characteristics under limited test parameters against other vegetable wastes [12], warranting further study. Various other products can also be produced from cabbage, such as bioadsorbents, nanofibrillated cellulose, dietary fibers, proteins, and other bioactive compounds, as cabbage stalks can have a protein content of 12–20 g per 100 g of dried cabbage stalk [4, 9, 11, 13–15]. However, the suitable valorization route will depend on local infrastructure, industry, and demand. Biochar is a simple product that is readily produced, easily transported, and with wide applicability.

The conditions for pyrolysis, such as temperature, particle size of biomass, shape, holding time, and heating rate, have a significant influence on the structural and physicochemical properties of biochar [16, 17]. Temperature is the most influential parameter, as it drives the degree of carbonization and elemental changes. Other factors are important in defining kinetics and heat transfer within the biomass. Typically, holding time and heating rate are studied and their effects are reasonably well known [18]. On the other hand, particle size and biomass quantity, which affect surface area and both heat and mass transfer, are relatively under-studied. Particle size has been demonstrated to impact yield [16] as well as various biochar properties such as elemental composition, specific pore volume, surface area, electrical conductivity, and surface functional groups [19], while we were unable to find any studies relating to the effect of biomass quantity. It is quite possible that the larger particle size and quantity of biomass may hamper heat transfer during pyrolysis, particularly in

fixed bed systems, and ultimately this may result in a reduced carbon content of char [17]. Keeping these aspects in view, a preliminary investigation is required at laboratory scale to find out the most suitable pyrolysis temperature, particle size, and quantity of biomass to produce best char suitable for soil amendment. Particle size is also a critical parameter to improve drying of the raw feedstock which can be done by solar drying or low-grade heat from the flue gas, given cabbages high moisture content. Wet biomass is difficult to macerate to very small sizes, although it is expected that smaller sizes will improve drying and biochar properties. Hence, selecting a single size that is both suitable for a drying pretreatment and to produce a biochar of desirable characteristics is important for economic considerations.

Various physicochemical properties of biochar like ash content, pH, electrical conductivity (ECE), zeta ( $\zeta$ )-potential, carbon (C), nitrogen (N), and cation exchange capacity (CEC) are major influencing properties that can influence the performance and suitability for various plants and soils. These properties of biochar when mixed with soil affect soil fertility, soil microbial community and associated nutrient turnover, plant germination, and plant growth [1]. Currently, only a handful of studies report production of biochar from cabbage and only present limited characterization [20, 21]. Optimization through response surface methodology (RSM) is an effective tool to understand the interaction between the factors used to produce biochar and their significance through different responses [22]. RSM with a combination of central composite design (CCD) is a well-established structure to improve effectiveness of modeled factors [23]. The objectives of this study are, therefore, to evaluate the effect of three key pyrolysis parameters: temperature, quantity of biomass, and feedstock size, on the various biochar characteristics for a cabbage-waste-derived biochar; and confirm via planting test with *Ipomoea purpurea* that biochar produced under these conditions is a suitable soil amendment agent.

## 2 Materials and methods

### 2.1 Experimental design

For use of biochar as a soil amendment, understanding and predicting its physical and surface-chemistry characteristics are important to know how it will function and influence the physicochemical properties of soil [24]. To understand how the biochar preparation parameters influenced these final characteristics, the experiment was designed by RSM. Optimum response of biochar was determined by the correlation between the responses (biochar yield, ash content, pH,  $\zeta$ -potential, ECE, CEC, C, N, and fixed carbon (FC)) and the quantitative experimental variables (heating temperature, sample sizes, and mass of feed biomass).

The temperature range selected was 300–600 °C, based on the range reported in most studies and the temperature region that typically shows the most variation and most suitable characteristics for agriculture [12]. Particle sizes from other studies typically range from 75 µm up to a few mm in diameter [16, 19]. Since cabbage is likely to be macerated prior to solar drying, we chose the upper region of this range to focus this study, selecting particles retained on sieves from 0.7 mm up to 2.4 mm in aperture size. Biomass feedstock masses ranged between 40–80 g, based on what was suitable for our fixed bed pyrolysis system.

The major aim of using RSM is to efficiently determine the optimal response through regression analysis of the response surfaces using the minimum experiments through factorial combination [25]. CCD is able to fit first-order and second-order linear degree models with the aid of the axial and central points. CCD analysis was conducted in Design-Expert 11 using a small central composite design with six repeated central points and replicate axial points. Orthogonality and curvature were estimated through CCD to minimize the variation in the regression coefficients [26, 27]. A CCD composed of a two-level factorial design and center point experiments (0, 0) was employed, consisting of 20 runs (Table 1). The span from factorial point design space to the center point was taken + 1 or - 1 and from the center to the star points as alpha  $|\alpha| = 1.667$ .

For particle size, an exact factorial and star point design could not be achieved due to standard sieve sizes. Hence, for modelling purposes, the sieve sizes 0.7, 1.0, 1.4, 2.0, and 2.4 were modelled as 0.67, 1.0, 1.5, 2.0, and 2.33, respectively, which are all within 7% of the true value. Given the range and unknown distribution of particle size in between each sieve, this approximation is reasonable.

The model fit was assessed by optimizing the adjusted  $R^2$  and corrected Akaike information criterion (AICc) separately, which was then compared for various other diagnostic and fit indices to evaluate the preferred model between these two. The prediction power was assessed with the adjusted  $R^2$ , as well as using the predicted vs actual plot which also confirmed whether residuals were randomly distributed and therefore the suitability of the model assumptions. Cook’s distance was used to identify influential and possibly erroneous measurements. Certainty of the model and remaining coefficients was

evaluated by the ANOVA  $p$  value. Notable interactions were identified by the magnitude of the interaction terms in the quadratic models, the shape of the surface plots, and the relative magnitude of the two independent variables in perturbation plots.

Optimization of the CCD-derived data was done using the Design Expert 11 optimize function. This was done with selected weighting towards certain parameters, along with their objective (minimize, maximize, constrain in a range) as indicated in Table S1. The optimization function creates a desirability function based on the parameter weighting that it then tries to maximize. To avoid local maxima, it uses 30 starting points across the design space.

### 2.2 Vegetable waste collection and biochar preparation

Waste cabbage was collected from a large university cafeteria at Qatar Foundation, Doha, Qatar. The large cabbage leaves were cut into smaller pieces with a range of 1 to 2 cm. Thereafter, the samples were dried at a temperature of 75 °C in a mechanical convection laboratory oven for 24 h [28]. This temperature was selected for drying of the feedstock because it is representative of solar drying [29] or low energy grade flue gas drying.

After estimating the weight of dried biomass, it was crushed into small pieces to reduce the biomass size before its pyrolysis. The crushed dry biomass was sorted into size groups retained by each of five standard sieves of size 0.7, 1, 1.4, 2, and 2.4 mm by following the ASTM standard D 422-63 [30] using a Haver EML Digital Plus (Haver & Boeker). Pyrolysis was conducted at a ramp rate of 5 °C min<sup>-1</sup> and a hold duration of 15 min using a muffle furnace (Lindberg Blue M-3504, Thermo Scientific) to produce biochar following the CCD structure (Table 2). These pyrolysis conditions result in high yields and suitable properties for soil amendments [17, 19].

### 2.3 Biochar characterization

After pyrolysis, the yield percentage of produced biochar was determined by Eq. 1 [1].

**Table 1** Coded and experimental variables for CCD

Coded variable	Experimental variable	Units	Coded level and actual level				
			-α	- 1	0	+ 1	+α
A	Set point temperature	°C	300	360	450	540	600
B	Sample size	mm	0.67	1.00	1.50	2.00	2.33
C	Sample mass	g	40	50	65	80	90

**Table 2** CCD run order of experiment design and experimental results

Actual run	Standard run	Temperature (°C)	Size (mm)	Quantity (g)	Yield (%)	pH	Zeta (mV)	ECE (mS.cm <sup>-1</sup> )	CEC (cmol <sub>e</sub> .kg <sup>-1</sup> )	C (%)	N (%)	FC (%)	Ash (%)	H/C	O/C
1	1	540	2.00	50	19.56	13.37	-56.3	0.582	17.56	64.77	2.23	44.77	21.95	0.004	0.196
2	6	360	2.00	80	23.93	7.50	-2.5	0.456	22.84	60.36	2.58	51.51	12.35	0.006	0.361
3	11	450	0.67	65	21.00	12.39	-58.2	0.561	24.52	64.73	2.61	46.24	18.84	0.005	0.215
4	16	450	1.50	65	22.26	12.00	-50.2	0.434	19.85	63.14	2.36	46.18	18.69	0.006	0.210
5	10	600	1.50	65	17.60	13.48	-49.3	0.401	16.38	75.18	2.30	63.41	22.35	0.001	0.184
6	20	600	1.50	65	16.78	11.76	-46.2	0.396	16.38	75.16	2.38	63.38	22.31	0.001	0.190
7	15	450	1.50	65	22.08	12.55	-65.1	0.435	19.72	63.03	2.31	46.32	18.61	0.006	0.218
8	9	300	1.50	65	28.09	7.10	-2.02	0.298	23.10	58.44	2.58	46.99	11.76	0.017	0.350
9	2	540	2.00	50	19.48	13.25	-51.2	0.575	18.35	64.71	2.28	45.57	21.25	0.004	0.128
10	17	450	1.50	65	22.11	12.48	-53.4	0.461	18.75	63.29	2.42	46.24	18.63	0.006	0.249
11	19	450	1.50	65	22.34	12.20	-56.1	0.470	19.70	63.32	2.45	46.20	18.71	0.006	0.049
12	5	360	2.00	80	23.80	7.80	-2.87	0.464	21.07	62.31	2.63	51.57	12.29	0.006	0.337
13	13	450	1.50	40	20.40	12.42	-45.2	0.426	19.83	63.26	2.34	46.32	18.61	0.006	0.266
14	18	450	1.50	65	21.75	12.25	-40.8	0.439	19.80	63.34	2.32	46.25	18.64	0.006	0.049
15	7	360	1.00	50	23.52	8.06	-1.35	0.399	25.16	62.97	2.75	51.21	12.82	0.005	0.335
16	12	450	2.33	65	22.88	12.10	-34.2	0.645	18.75	63.05	2.24	47.38	17.35	0.006	0.320
17	8	360	1.00	50	23.64	8.10	-1.74	0.384	25.20	62.54	2.86	51.49	12.84	0.006	0.329
18	4	540	1.00	80	19.30	13.45	-58.2	0.546	18.73	67.51	2.35	45.72	22.17	0.003	0.120
19	3	540	1.00	80	19.18	13.28	-66.7	0.482	18.57	66.24	2.30	42.30	25.53	0.003	0.132
20	14	450	1.50	90	21.39	11.80	-45.8	0.422	17.74	63.37	2.39	46.26	18.55	0.006	0.328

Yield of biochar (%)

$$= \frac{\text{Weight of biochar (g)}}{\text{Weight of oven dried wastes (g)}} \times 100 \quad (1)$$

The estimation of pH and ECE of biochar were performed using a calibrated pH meter (Orion Star A121) and conductivity meter (A329, Thermo Scientific). A mixture of biochar and ultrapure water ( $R = 18.2 \text{ m}\Omega$ ) in the ratio of 1:5 was put into the shaker at 150 rpm for 1 h before estimation of the pH and ECE [31, 32]. The measurement of CEC was performed following the ammonium acetate method [33].  $\zeta$ -potential was measured using a Malvern Zetasizer Nano-ZS [34]. A combustion type elemental analyzer (EA 3000, Eurovector) was used to determine C, H, and N content of biochar. The instrument was set with a furnace temperature of 980 °C and carrier flow of 121 mL min<sup>-1</sup>. Before analysis, the biochar samples were oven-dried. Samples ranging from 0.50 to 1.5 mg were weighed and acetanilide was used as a reference standard. Proximate analysis was conducted to measure FC and ash content of biochar following the American Society for Testing and Materials (ASTM) D7582-15 method [35]. The thermal analysis of the biochars was performed by using an SDT-2960 simultaneous DSC-TGA thermal analyzer (TA instruments).

The FC and the percentage of oxygen (O) contents were measured by the following equations, (2) and (3):

$$\text{FC}(\%) = 100 - [\text{Ash}(\%) + \text{Volatile matter}(\%)] \quad (2)$$

$$\text{O}\% = 100 - (\text{C}\% + \text{H}\% + \text{N}\% + \text{Ash}\%) \quad (3)$$

## 2.4 Planting pot test studies

After analyzing the optimum conditions for producing biochar, pot tests were conducted using unplanted and planted pots filled with a mixture of sand and biochar produced at the optimum pyrolysis temperature and size. Unplanted and planted plastic pots of 9 cm (W × L) by 16 cm (D) were filled with 400 g of loamy sand, which contains 73.6% sand, 15.7% silt, and 16.2% clay amended with 0% (control) and 2% (w/w) biochar. A fraction of 2% biochar was chosen based on our own unpublished results with sand and other literature [36]. The loamy sand, commonly used in Qatar, was collected from our university landscaping department. For planting tests, *I. purpurea* was selected as it can survive in high temperature and is widely grown as an ornamental plant in Qatar. Ten seeds of *I. purpurea* were placed in each container in a similar manner. Replicates of each unplanted and planted pot were monitored for 10 days. Water supply, water evapotranspiration, and water retention of unplanted and planted pots were recorded daily (24 h intervals) based on the weight changes of the pots before and after watering. During these periods, plant

growth was measured on the basis of seeds germinated, plant height, and number of leaves.

## 2.5 Statistical analysis of plant growth

The statistical significance of changes in plant growth and water retention capacity at different rates of biochar application were determined using two-way independent analysis of variance (ANOVA) where the second two-level factor was the day of measurement. Significance was defined at  $\alpha = 0.05$ . The analysis was conducted using the IBM SPSS statistical package.

## 3 Results and discussion

### 3.1 Model factor variations of biochar

#### 3.1.1 Yield

After pyrolysis, the yields of biochar at different pyrolysis temperatures were analyzed and presented by RSM (Fig. 1). The yield of biochar is plotted against the three design factors: temperature, biochar size, and quantity of feed in Fig. 1a and b. The yield is maximum at the lowest temperature tested of 300 °C and medium size of 1.50 mm (Fig. 1a). The yield reduced from 28.09% under optimum conditions to a minimum value of 17.60% for the tested conditions at the highest pyrolysis temperature. Temperature was the most influential factor on biochar yield due to the conversion of lower weight molecular organics into the gaseous form [37]. The most notable interaction was between particle size and mass, where an opposite response to feedstock mass was observed at small and large particle sizes. This is likely due to a complex relationship between heat transfer, heat retention, and biomass decomposition. Smaller particle size and mass lead to more

rapid heating and cooling, the latter being particularly important given the relatively short hold time (15 min), since the furnace and sample cooled naturally following the hold period. The degradation of cellulose to a more stable anhydrocellulose, which gives higher biochar yield, is the dominant reaction at higher temperature and cellulose depolymerizes producing volatiles. During the pyrolysis process, carbonaceous volatiles are driven off, and their escape from the sample through the particles and between particles can drive subsequent reactions, which are influenced by the particle size and mass.

It is obvious from the perturbation plot (Fig. S1a) that the relative effect of temperature (A) was much more significant than either particle size (B) or mass (C). The final quadratic model did not include a quadratic term for particle size or interaction between temperature and particle size (Table S3). It had an  $R^2_{adj}$  value of 0.984 and model ANOVA  $p$  value of  $< 0.0001$  (Table S4) with well distributed residuals (Fig. S1b).

#### 3.1.2 Ash content and pH

The response surface plots for ash content and pH based on the pyrolysis temperature, particle size, and quantity of biomass feed are presented in the Fig 2. The ash content of feedstock was 8.4%. Biochar ash content was highly influenced by pyrolysis temperature, whereas particle size and mass had minimal impact (Fig. 2, Fig. S2). Biochar at the highest temperature had the highest ash content due to the loss of carbonaceous volatiles. Beyond the main effects, the model for ash only contained the quadratic term for temperature and interaction term for particle size and mass (Table S3). The model had an  $R^2_{adj}$  of 0.965 along with an ANOVA model  $p$  value of  $< 0.0001$  (Table S5) which shows model suitability based on the predicted versus experimental data (Fig. S2b). The modeled equation developed for ash content is given in Eq. 5 (Table S3).

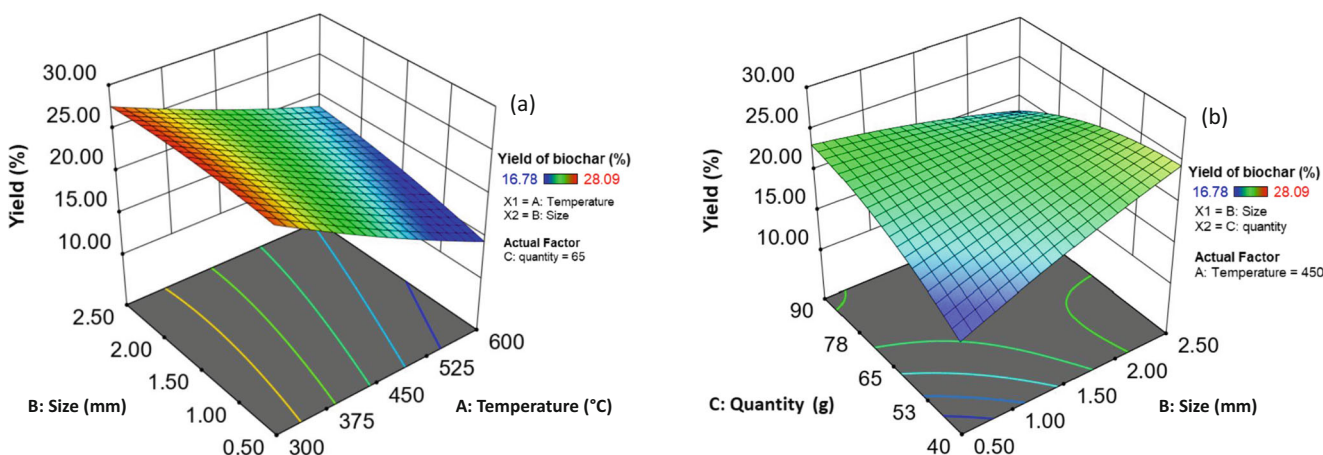
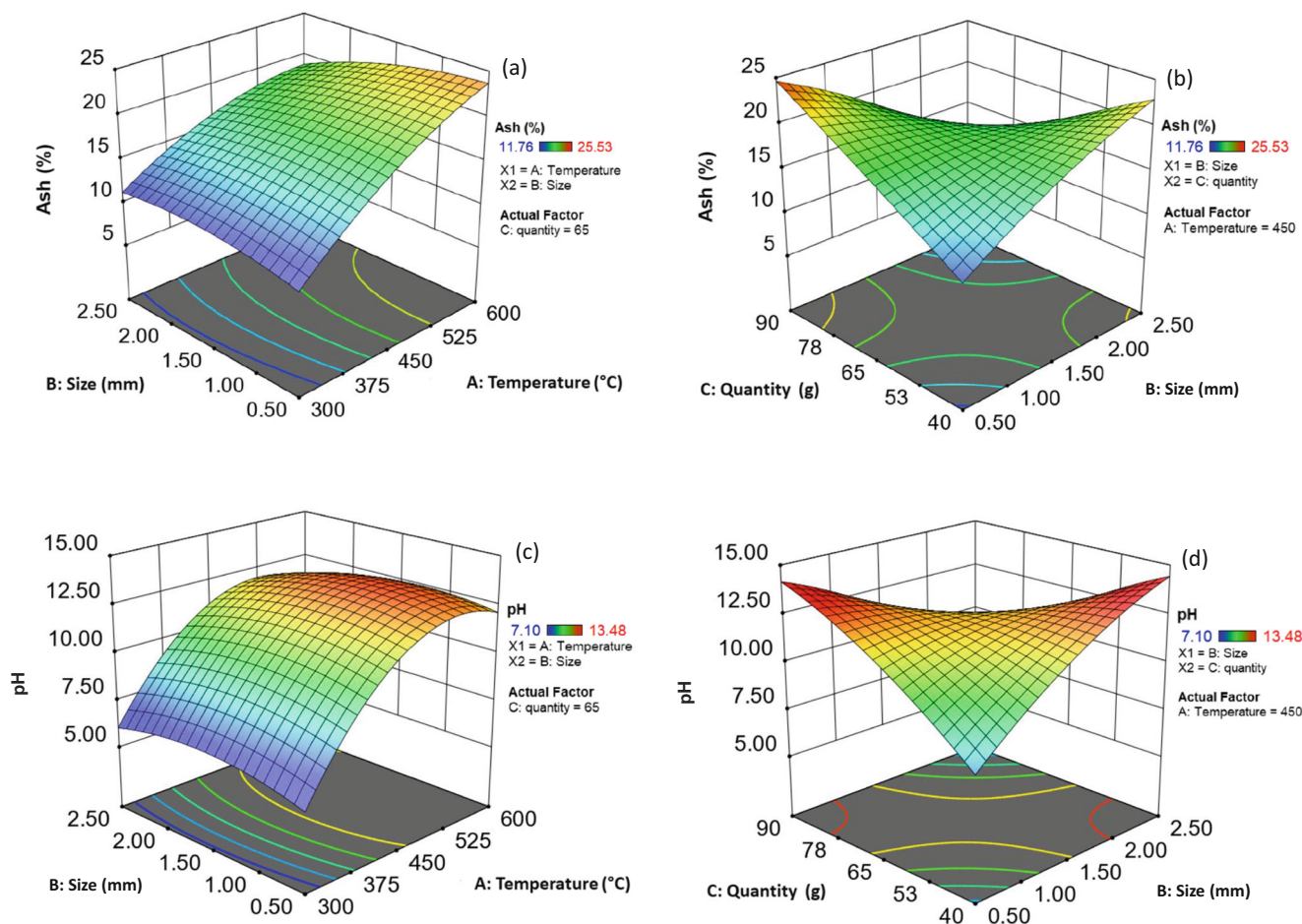


Fig. 1 3-D surface response for yield of biochar with the design factors: (a) temperature and size and (b) size and quantity



**Fig. 2** 3-D surface response for (a, b) ash content and (c, d) pH of biochar with the design factors temperature, size and quantity

The pH was also strongly influenced by increasing temperature (Fig. 2 c and d), and showed strong correlation with ash content. The pH of all produced biochars was more than 7, signifying the alkaline nature of the biochar (Fig. 2c). The maximum response for pH (13.5) was observed at a temperature of 600 °C and was near neutral at a temperature of 300 °C. For biochar application in desert sands, which have a pH between 5.5 and 7, the use of a slightly alkaline biochar is effective to balance the pH and promote germination and plant growth [38]. Junna et al. [39] reported biochar at a range of pH 7 to 8 amended with soil preferably increases CEC of saline soil and plant growth in comparison to biochars with higher pH, which is similar to the biochar produced at 360 °C in our study.

The combined effect of particle size and quantity of feed biomass on the pH is shown by the response curve in Fig. 2d. For a small particle size and a large quantity, as well as a large size and small quantity, a slightly higher pH was observed. However, it is clear from the perturbation plot (Fig. S2c) that these two factors had minimal overall impact on the pH, while temperature was the main driver. The final model therefore

contained linear and quadratic terms for temperature, the linear components of particle size and mass (which were insignificant) and their interaction term. The model had an ANOVA  $p$  value < 0.0001 (Table S6) and an  $R^2_{adj}$  of 0.934, showing a suitable prediction tool in agreement with the experimental data (Fig. S2d). The modeled equation developed for pH is given in Eq. 6 (Table S3).

### 3.1.3 $\zeta$ -potential

$\zeta$ -potential denotes the net charge between the surface plane and slip plane of a colloidal particle. The negative charge of  $\zeta$ -potential was observed to increase with increasing pyrolysis temperature up to 540 °C, after which it decreases again (Fig. 3a). Figure 3b shows that  $\zeta$ -potential is also influenced by the particle size and feedstock mass, where low values or high values of both these factors lead to less negative  $\zeta$ -potential charges. This was particularly true for a large size and quantity.

Xue et al. [40] reported in their study that biochar produced from different types of leafy vegetable wastes including stems

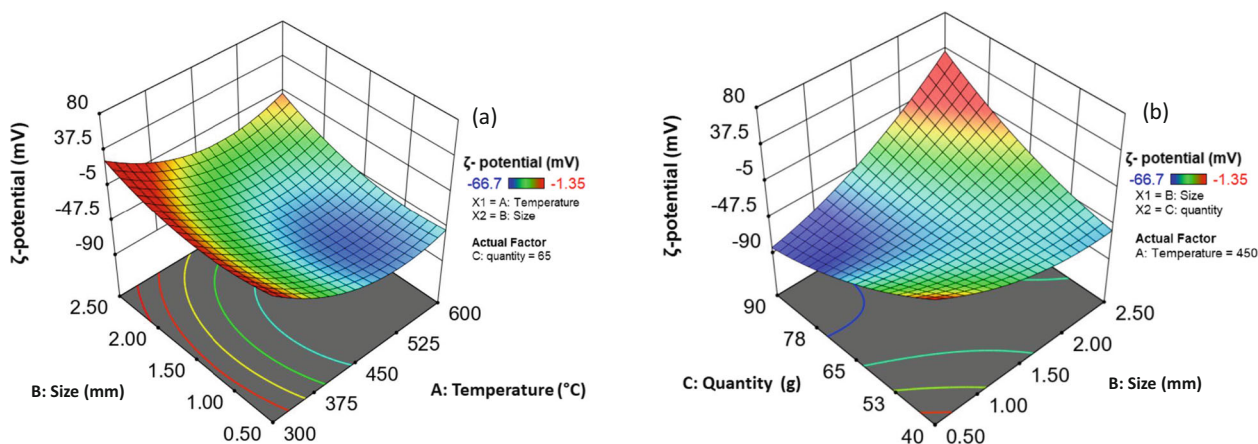


**Fig. 3** 3-D surface response for  $\zeta$ -potential of biochar with the design factors (a) temperature and size of feedstock and (b) size and quantity of feedstock

had a maximum negative  $\zeta$ -potential of  $-51.5$  mV produced at  $400$  °C. A comparable observation was made in our study for  $450$  °C and a particle size  $0.67$  ( $-53.6$  mV). However, the optimum  $\zeta$ -potential of cabbage waste biochar was  $-66.7$  mV at  $540$  °C in our study. An increasing negative  $\zeta$ -potential is in good agreement with increasing pH [41], which was also observed (Fig. 2). The strong relationship with temperature is likely due to the changing surface groups and increasing porosity caused as temperatures rise. Up to around  $480$  °C, the acidic functional groups like phenolic and carboxylic acid remain on the biomass, but within the  $350$ – $650$  °C range, significant transformations of the functional groups occur [42], as evident by FTIR spectra (Fig. S3).

A curvature from the perturbation plot was observed for all the three design factors, with temperature as the most influential factor, but both particle size and mass also influencing the  $\zeta$ -potential (Fig. S4a). A good correlation between predicted values and actual experimental values of  $\zeta$ -potential was achieved as shown in Fig. S4b. The final quadratic model of  $\zeta$ -potential contained all main effects and their quadratic terms, but only an interaction between mass and particle size. The model had an  $R^2_{\text{adj}}$  of  $0.983$  and an ANOVA  $p$  value of  $< 0.0001$  (Table S7), indicating a relatively good prediction tool for  $\zeta$ -potential. The adequate precision ratio was the one of the two lowest among the models, but at  $14.8$  is still very acceptable. Temperature is again the most significant factor although a high degree of interaction was observed between particle size and adsorbent mass. The quadratic equation developed due to modeled factors for  $\zeta$ -potential is presented in Eq. 7 (Table S3).

### 3.1.4 ECE

The ECE of biochar is important as it indicates the biochar's salinity and directly affects seed germination and plant

growth. High salinity is a major contribution to the loss of growth yield and productivity in cultivated lands [43]. The ECE values of biochar produced from cabbage by different pyrolysis temperatures remained less than  $0.8$  mS  $\text{cm}^{-1}$  (Fig. 4a), which is effective for the germination of plants and plant growth [43]. The response of ECE showed an optimum (minimum) at the lowest temperature and was maximal between  $450$  and  $600$  °C.

Particle size had a much stronger effect on ECE than most other response variables, with a minimum ECE at intermediate particle sizes. This is likely due to the heat transfer effects related to particle size influencing both heating and cooling, and consequently defining the exact transformations taking place both at the surface and internally in the biochar particles. Mass had little direct effect on ECE but had interactions with both temperature and particle size (Fig. 4b). While this appeared relatively significant, it should be noted that both axial points for particle size had large Cook's distance of  $> 3$ , making these edges of the response surface plot highly influenced by these two measurements. The predicted quadratic equation for ECE has an  $R^2_{\text{adj}}$  of  $0.907$  with an ANOVA  $p$  value of  $< 0.0001$  (Table S8), indicating a highly suitable prediction tool. The quadratic model equation is shown in Eq. 8 (Table S3).

### 3.1.5 CEC

CEC is a measure of a soil's ability to hold positively charged ions and influences soil structure stability, nutrient availability, pH, and the interaction with cations and anions. The optimum (largest) CEC value was observed at the lowest pyrolysis temperature of  $300$  °C and smallest particle size. It decreased linearly with increasing temperature, particularly for larger particle sizes (Fig. 5a). Increasing the pyrolysis temperature reduces the CEC of biochar, and the optimum CEC of biochar at low temperature may arise due to the presence of

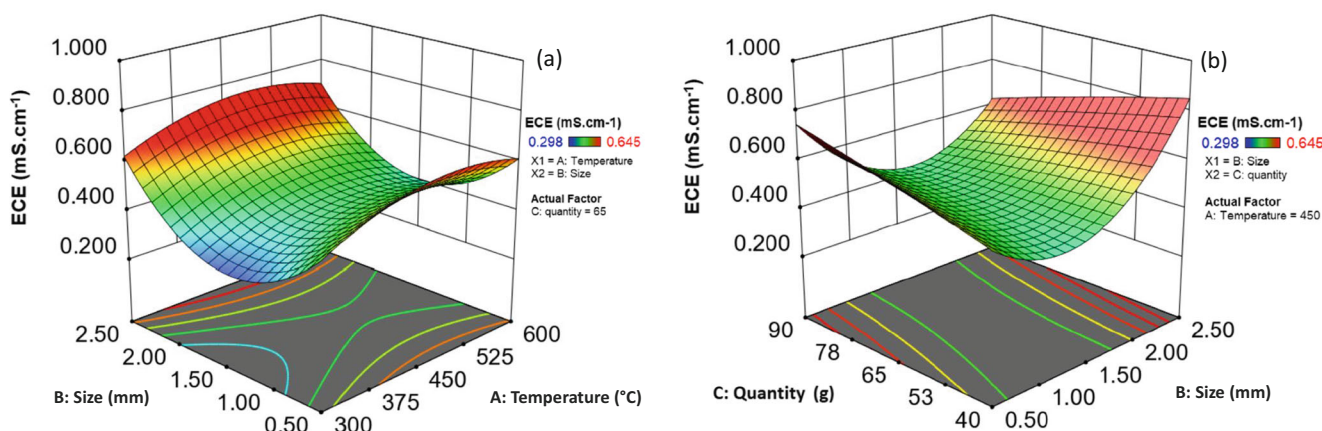


**Fig. 4** 3-D surface response for ECE of biochar with the design factors (a) temperature and size of feedstock and (b) size and quantity of feedstock

non-carbonized organic matter containing functional groups (Fig. S4) and low aromatic character [44].

Particle size showed a strong nonlinear effect on CEC with a minimum in the region of 2 mm (Fig. 5), though there was no significant increase at higher temperature. The cation exchange capacity is primarily associated with negatively charged functional groups such as hydroxyl, carbonyl, and carboxyl. These are more prevalent at lower temperatures and are driven off at higher temperatures. Since decomposition and volatilization of these compounds occurs more readily at the surface, these groups disappear more quickly for smaller particles sizes, and corresponded well with observed O/C ratios. However, CEC is also strongly influenced by surface area, which at low temperatures is going to be more influential due to the presence of these functional groups, as seen by the difference in response to particle size at low vs high temperature (Fig. S6). Mass had a linear influence on CEC with higher CEC at smaller mass and could be related to the longer cooling time associated with higher mass.

The quadratic model fitted to the experimental data contained all main effects, a quadratic term for particle size and interactions involving mass. It had an  $R^2_{adj}$  of 0.9389 and a model ANOVA  $p$  value of  $< 0.0001$  (Table S9). The quadratic modeled equation is given in Eq. 9 (Table S3). Biochars with CEC in this range of 25–30 cmol kg<sup>-1</sup> are beneficial as this is at least two-thirds more than the CEC for most sandy soils [45].

### 3.1.6 C, N, and FC

Mineralization and immobilization rates in biochar are a function of C and N [46]. The surface response of C and N with the three different model factors (temperature, particle size, and quantity) of feed biomass is shown in Fig. 6. C and FC content increased with temperature, achieving maximum values at 600 °C. In contrast, N content showed a reverse response, with maximum content at low temperature (Fig. 6c–d). This is due to the more volatile nature of most nitrogen compounds, such as proteins, compared to many of the organics such as cellulose.

Neither particle size nor mass had almost any main effect on carbon content of the biochar or influence on the response

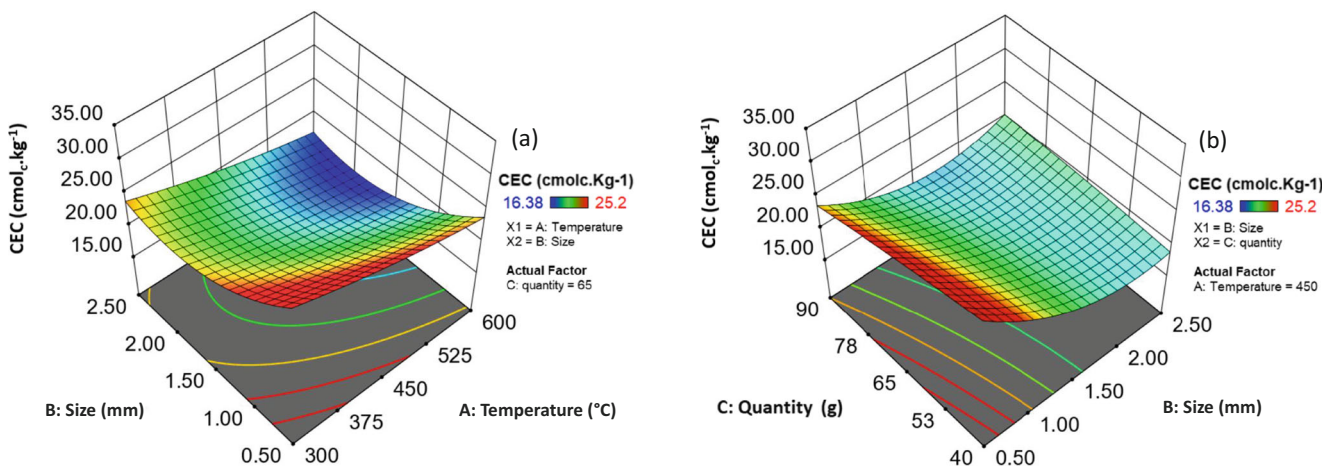


**Fig. 5** 3-D surface response for CEC of biochar with the design factors (a) temperature and size of feedstock and (b) size and quantity of feedstock



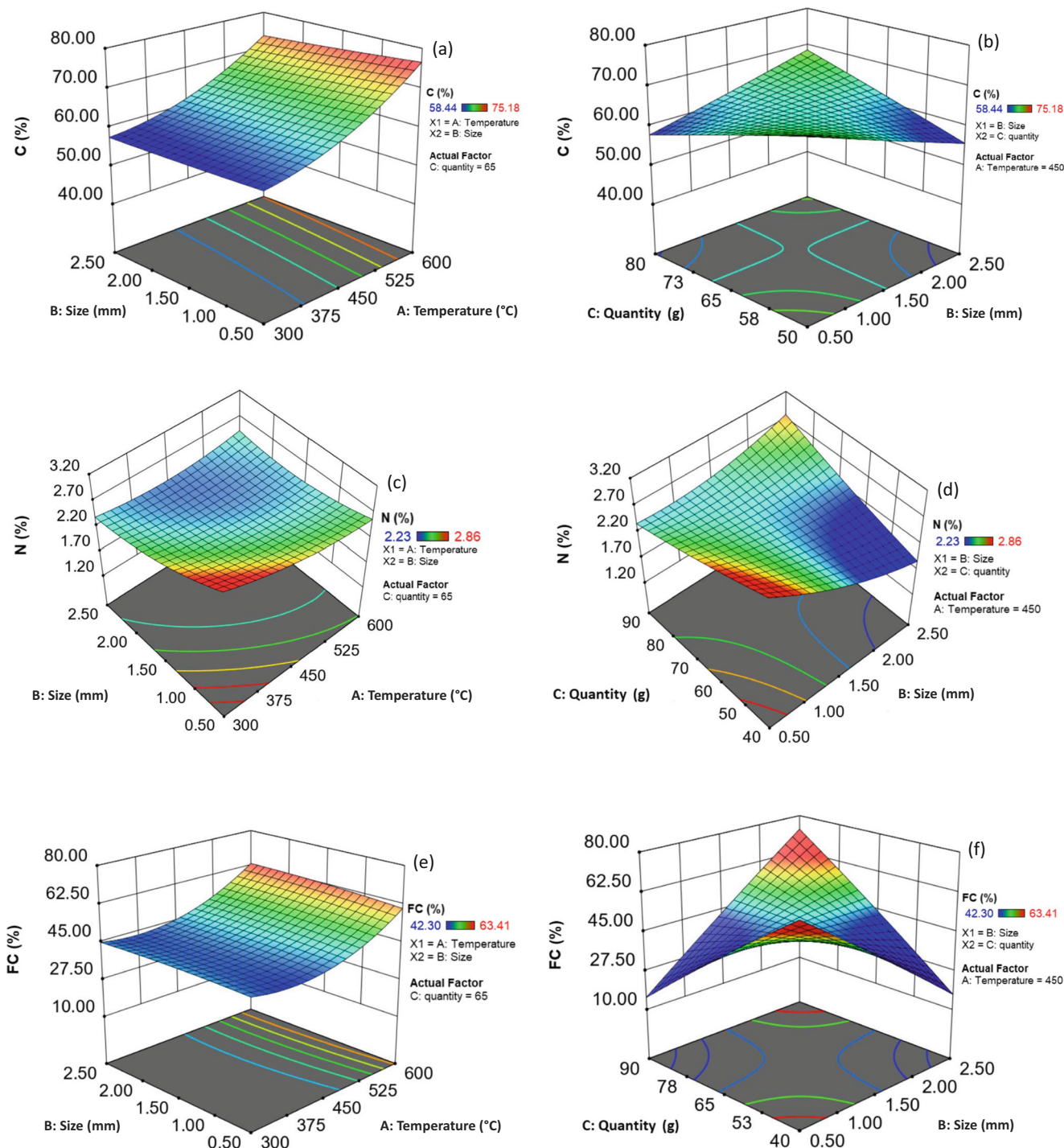


**Fig. 6** 3-D surface response (a, b) for C, (c, d) for N, and (e, f) for FC of biochar with the design factors temperature, size, and quantity of feedstock

to temperature, but did show some interaction with each other. However, particle size did influence N content, with smaller particle size resulting in a higher proportion of N. This may be due to decreased mass transfer resistance at smaller particle size (larger surface area) that has a more pronounced effect on the rate of release of larger molecules containing H and O (e.g., CO<sub>2</sub>, CH<sub>4</sub>) compared to NH<sub>3</sub>. Higher C and lower N values imbalance the C and N value of soil and can cause poor

crop growth and soil fertility [47, 48]. Biochar produced at low temperature and particle size results in an optimum response of N. The perturbation plot in Fig. S7 provides the response change of the three factors demonstrating temperature as the most influential factor, followed by particle size.

The models for C and FC contained a quadratic term for temperature, along with main linear components for all factors and an interaction term for particle size and mass, though mass

was not a significant predictor for either C or FC and particle size was only significant for C. For N, the optimum model also included a quadratic term for particle size. Actual measured values vs model-predicted response of C, N, and FC is shown in Fig. S7. The fits were good for C and FC, while N showed the largest deviations and lowest adequate precision of any response factor, although still reasonable at 14.2. The  $R^2_{\text{adj}}$  values for C, N, and FC model are 0.967, 0.847, and 0.951, respectively. All these models showed an ANOVA  $p$  value of  $< 0.0001$ , indicating that the models are suitable to explain the variance in the data (Table S10 to S12). The quadratic model equations developed for C, N, and FC are given in Eq. 10–12 (Table S3).

It should also be noted that all biochar produced had H/C lower than 0.02 and O/C less than 0.36, except at 300 °C which had an O/C of 0.45 (Fig. S8). These low H/C values indicate that biochar meets the stability requirements of the International Biochar Association standards to be classed as a biochar and thermochemically processed material [49].

### 3.2 Process optimization and model confirmation

The vital part of the present work is to determine the characteristics of cabbage-derived biochar and the optimum pyrolysis conditions to make it as an effective soil amendment agent for enhanced plant growth and water retention capacity. The optimum temperature, size, and quantity of the feedstock were determined mathematically using weighted optimization based on overall desirability. The weighting factors are provided in Table S1 and prioritized yield (weighting 5), followed by pH, CEC, and elemental composition (all weighting 4), with  $\zeta$ -potential given the lowest priority (weighting 3). Twelve local optima were identified (Table S13) which all showed very similar temperature (361.1–362.8 °C), particle size (0.88–0.98 mm), and feedstock mass (40.88–44.38 g).

These conditions indicate that generally speaking, for cabbage biochar, relatively lower temperature, smaller particle size, and smaller mass of feedstock enhance most properties of the biomass. The optimal biochar based on the weighted desirability function had a yield of 22.2%, pH of 8.00,  $\zeta$ -potential of  $-1.35$  mV, ECE of  $0.36 \text{ mS cm}^{-1}$ , CEC of  $25.35 \text{ cmol kg}^{-1}$ , C content of 65.34%, N content of 2.88%, FC content of 58.18%, and ash content of 11.76%. The optimal point showed good overall properties with relatively high CEC, mildly alkali pH, and relatively low ECE. The optimal solution did show compromise on optimal zeta-potential, which was much less negative than at 540 °C, and had notably lower C and FC content and higher ECE than could be achieved if they were optimized as single target responses.

In general, the influence of feedstock mass was minimal on the biochar characteristics, though some interactions were observed with particle size indicating that surface area-driven heat and mass transfer factors have some role in the process. In general, a smaller mass of feedstock resulted in slightly improved conditions, e.g., for pH, ECE, CEC, C, N, and FC, although both yield and  $\zeta$ -potential were negatively impacted. The relatively small impact of feedstock mass is beneficial for scale up, while both particle size and temperature can be easily controlled in the process. The optimum conditions of a lower pyrolysis temperature are also beneficial from an energy and economic perspective.

The fit statistics for the various response variable models are provided in Table S14. The  $R^2_{\text{adj}}$  of all models was high, with all but N being greater than 0.9. The adequate precision ratios were all also significantly greater than 4. However, a number of models for response variables suffered from predicted  $R^2$  values more than 0.2 less than the  $R^2_{\text{adj}}$  values. These response variables were pH,  $\zeta$ -potential, ECE, CEC, and N, indicating that these particular models would not be

**Table 3** Different properties of biochar derived from different food wastes

Types of food wastes	Pyrolysis temperature used to produce biochar (°C)	Yield (%)	pH	$\zeta$ -potential (mV)	H/C:O/C	ECE ( $\text{ms cm}^{-1}$ )	CEC ( $\text{cmol}_c \text{ kg}^{-1}$ )
<sup>1</sup> Cassava	600	31.44	$8.5 \pm 0.3$	-	-	$3.24 \pm 0.1$	$19.44 \pm 0.5$
<sup>1</sup> Corn cob	650	26.88	$11.0 \pm 0.5$	-	-	$0.73 \pm 0.1$	$16.85 \pm 0.5$
<sup>1</sup> Coffee husk	490	45.83	$8.0 \pm 0.3$	-	-	$0.79 \pm 0.1$	$12.52 \pm 0.5$
<sup>2</sup> Pea pods	300–600	22–5	$8.84 \pm 0.08$	-	0.1:0.7	$1.30 \pm 0.1$	$12.14 \pm 0.5$
<sup>2</sup> Cauliflower	300–600	30–14	$*9.84 \pm 0.011$	-	0.1:0.5	$1.31 \pm 0.1$	-
<sup>2</sup> Orange peel	300–600	25–18	$*9.43 \pm 0.17$	-	0.1:0.7	$0.238 \pm 0.2$	-
<sup>3</sup> Bean dregs	300–700	50.3–22.9	$*9.71 \pm 0.01$	*- 60.2	$< 0.01: < 0.2$	-	-
<sup>3</sup> Fruit pericarp	300–700	51.5–29.3	$*8.56 \pm 0.05$	*- 25.8	$< 0.07: < 0.4$	-	-
<sup>3</sup> Nut husks	300–700	58.4–30.4	$*8.14 \pm 0.12$	*- 46.6	$< 0.07: < 0.4$	-	-
<sup>3</sup> Stems/leafy vegetables	300–700	49.8–33.0	$*12.02 \pm 0.03$	*- 51.5	$< 0.08: < 0.3$	-	-
<sup>3</sup> Tea leaves	300–700	64.0–31.0	$*9.23 \pm 0.01$	*- 33.6	$< 0.09: < 0.3$	-	-

#: 300 °C; \*: 400 °C; 1:[50]; 2: holding rate  $10 \text{ °C min}^{-1}$  for 1 h [52]; 3: holding rate  $5 \text{ °C min}^{-1}$  for 2 h [41]

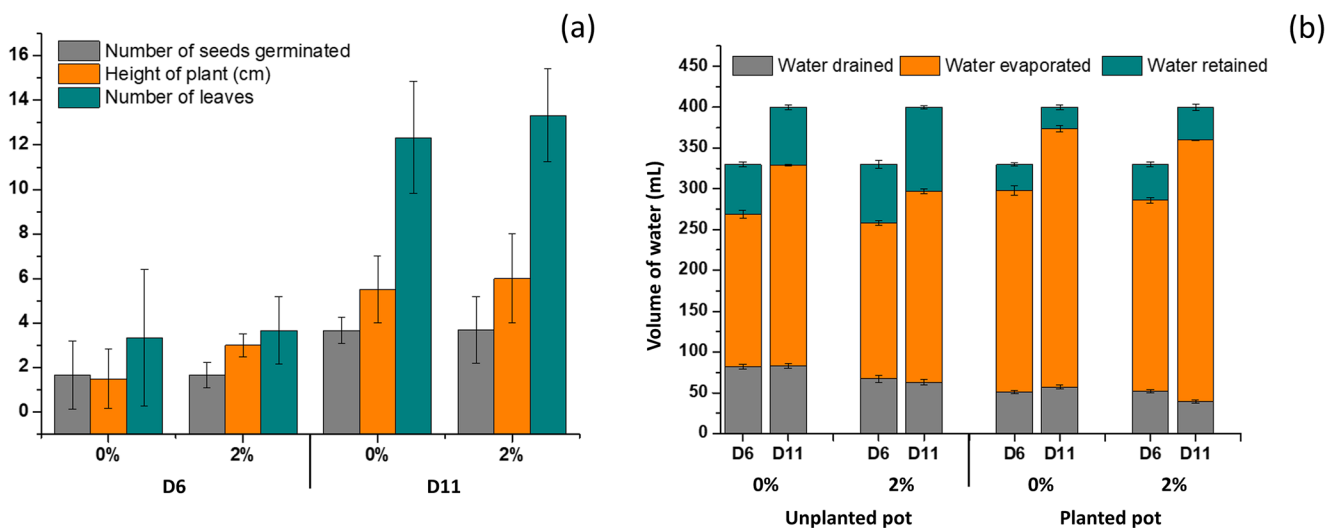


**Fig. 7** Pot confirmation test for the optimum conditions of biochar pyrolysis showing (a) *I. purpurea* plant growth and (b) water retention at 0% and 2% of biochar for 10 days of operation. Standard deviation shows the variation in replicates and D stands for days

suitable for making predictions of values due to the high variability in some experimental responses to the model.

The applicability of cabbage biomass as a feedstock of biochar was compared with other food waste biochar properties that is shown in Table 3 [50, 51]. The properties in general are similar to other feedstocks, although the yield is lower than most, due to the higher cellulose and lower lignin content of cabbage. The lowest pH biochar achieved with cabbage was more neutral than any other feedstock, including cauliflower which is the most similar feedstock and was measured over a similar temperature range. This makes it highly suitable for soil amendment. Cabbage biochar also proves favorable with regard to a low ECE and high CEC, indicating it has highly suitable agricultural properties.

### 3.3 Evaluation of optimum biochar on plant growth

Based upon model optimization, the biochar produced at 360 °C and nearest sieve size of 1.0 mm size was selected and tested on the ornamental plant *I. purpurea* to observe the plant growth and water retention capacity (Fig. 7). After 10 days of growth, an increase of 8.3% in average plant height and 7.5% in number of leaves was observed in 2% biochar pots compared to the control condition (Fig. 7a). However, neither result was statistically significant ( $p > 0.05$ ). The 2% biochar amended sand was also found effective to increase water retention from 18% in the control to 32% in the unplanted condition and from 6.5 to 10% in the planted condition ( $p = 0.016$  and 0.001, respectively) (Fig. 7b). Further confirmation planting studies are warranted for chars produced at different temperatures, particle sizes, and feedstock quantities in the region identified by optimization to fully confirm the predicted

process conditions. Long-term studies of biochar application with different plants and soils are also warranted.

## 4 Conclusion

This study demonstrates that biochar produced from cabbage waste has suitable characteristics for use as a soil amendment. The design factors of pyrolysis temperature, feed size, and quantity were analyzed. Of these, pyrolysis temperature is the most influential factor across all response characteristics, while feedstock particle size is also important. Mass provided little main effects but did cause interactions, notably with particle size. The biochar produced at optimum conditions had a relatively high CEC and moderately alkaline pH, making it desirable as a soil amendment. Due to the cellulose-rich nature of cabbage, it had relatively low yield and moderate carbon fraction. The optimum cabbage biochar found by RSM provided potential improvements in plant growth and water retention capacity of soil in the short preliminary planting study. This highlights the potential of this waste material for biochar soil applications and the need for further planting studies.

**Funding** The authors would like to thank Qatar National Research Fund for their support of this research through NPRP-11S-0117-180328, and co-funding from Qatar Supreme Committee for Delivery and Legacy through the Challenge 22 program.

### Compliance with ethical standards

**Conflict of interest** The authors have no conflicts of interest to declare. Any opinions, findings, conclusions, or recommendations expressed in this material are those of the author(s) and do not necessarily reflect the views of HBKU, QF, or Supreme Committee for Delivery and Legacy.

## References

- Zhao S, Ta N, Wang X (2017) Effect of temperature on the structural and physicochemical properties of biochar with apple tree branches as feedstock material. *Energies* 10:1293. <https://doi.org/10.3390/en10091293>
- Ahmadvand M, Soltani J, Hashemi Garmdareh SE, Varavipour M (2018) The relationship between the characteristics of biochar produced at different temperatures and its impact on the uptake of NO<sub>3</sub>-N. *Environ Health Eng Manag* 5:67–75. <https://doi.org/10.15171/EHEM.2018.10>
- Beniche I, Hungria J, El Bari H et al (2020) Effects of C/N ratio on anaerobic co-digestion of cabbage, cauliflower, and restaurant food waste. *Biomass Conv Bioref*. <https://doi.org/10.1007/s13399-020-00733-x>
- Sagar NA, Pareek S, Sharma S, Yahia EM, Lobo MG (2018) Fruit and vegetable waste: bioactive compounds, their extraction, and possible utilization. *Compr Rev Food Sci Food Saf* 17:512–531. <https://doi.org/10.1111/1541-4337.12330>
- FAO (Food and Agriculture Organization) (2014) Definitional framework of food losses and waste. Rome, Italy
- Laufenberg G, Schulze N (2009) A modular strategy for processing of fruit and vegetable wastes into value-added products. In: Waldron K (ed) *Handbook of Waste Management and Co-Product Recovery in Food Processing*. Woodhead Publishing, pp 286–353
- FAOSTAT (2019) Statistics for climate change in agriculture, forestry and other land
- Hossain MA, Ngo HH, Guo WS, Nguyen TV, Vigneswaran S (2014) Performance of cabbage and cauliflower wastes for heavy metals removal. *Desalin Water Treat* 52:844–860. <https://doi.org/10.1080/19443994.2013.826322>
- Sun X, Shan R, Li X, Pan J, Liu X, Deng R, Song J (2017) Characterization of 60 types of Chinese biomass waste and resultant biochars in terms of their candidacy for soil application. *GCB Bioenergy* 9:1423–1435. <https://doi.org/10.1111/gcbb.12435>
- Khukutapan D, Chiewchan N, Devahastin S (2018) Characterization of nanofibrillated cellulose produced by different methods from cabbage outer leaves. *J Food Sci* 83:1660–1667. <https://doi.org/10.1111/1750-3841.14160>
- Rutherford DW, Wershaw RL, Rostad CE, Kelly CN (2012) Effect of formation conditions on biochars: compositional and structural properties of cellulose, lignin, and pine biochars. *Biomass Bioenergy* 46:693–701. <https://doi.org/10.1016/j.biombioe.2012.06.026>
- Pradhan S, Abdelaal AH, Mroue K, et al (2020) Biochar from vegetable wastes: agro-environmental characterization. *Biochar* (in press). <https://doi.org/10.1007/s42773-020-00069-9>
- Brito TBN, Pereira APA, Pastore GM, Moreira RFA, Ferreira MSL, Fai AEC (2020) Chemical composition and physicochemical characterization for cabbage and pineapple by-products flour valorization. *LWT* 124:109028
- Collard F-X, Blin J (2014) A review on pyrolysis of biomass constituents: mechanisms and composition of the products obtained from the conversion of cellulose, hemicelluloses and lignin. *Renew Sust Energ Rev* 38:594–608
- Herranz J, Vidal-Valverde C, Rojas-Hidalgo E (1981) Cellulose, hemicellulose and lignin content of raw and cooked Spanish vegetables. *J Food Sci* 46:1927–1933. <https://doi.org/10.1111/j.1365-2621.1981.tb04521.x>
- Demirbas A (2004) Effects of temperature and particle size on biochar yield from pyrolysis of agricultural residues. *J Anal Appl Pyrolysis* 72:243–248. <https://doi.org/10.1016/j.biortech.2012.10.150>
- Yadav K, Jagadevan S (2019) Influence of process parameters on synthesis of biochar by pyrolysis of biomass: an alternative source of energy. *Recent Adv Pyrolysis*. <https://doi.org/10.5772/intechopen.88204>
- Zhao B, O'Connor D, Zhang J et al (2018) Effect of pyrolysis temperature, heating rate, and residence time on rapeseed stem derived biochar. *J Clean Prod* 174:977–987. <https://doi.org/10.1016/j.jclepro.2017.11.013>
- Abbas Q, Liu G, Yousaf B, Ali MU, Ullah H, Munir MAM, Liu R (2018) Contrasting effects of operating conditions and biomass particle size on bulk characteristics and surface chemistry of rice husk derived-biochars. *J Anal Appl Pyrolysis* 134:281–292. <https://doi.org/10.1016/j.jaap.2018.06.018>
- Cheng J, Liu Y, Li Y et al (2018) Preparation of high contents of pyridinic and pyrrolic-nitrogen doped activated-carbon from pyrolysis of purple cabbage for the catalysis of oxygen reduction reaction. *Int J Electrochem* 13:11203–11214. <https://doi.org/10.20964/2018.11.81>
- Jo JH, Kim SS, Shim JW, Lee YE, Yoo YS (2017) Pyrolysis characteristics and kinetics of food wastes. *Energies* 10:1191. <https://doi.org/10.3390/en10081191>
- Campos LMA, Moura HOMA, Cruz AJG, Assumpção SMN, de Carvalho LS, Pontes LAM (2020) Response surface methodology (RSM) for assessing the effects of pretreatment, feedstock, and enzyme complex association on cellulose hydrolysis. *Biomass Conv Bioref*. <https://doi.org/10.1007/s13399-020-00756-4>
- Jitjammong J, Thunyaratchatanon C, Luengnaruemitchai A, Kongrit N, Kasetsomboon N, Sopajarn A, Chuaykarn N, Khantikulanon N (2020) Response surface optimization of biodiesel synthesis over a novel biochar-based heterogeneous catalyst from cultivated (*Musa sapientum*) banana peels. *Biomass Conv Bioref*. <https://doi.org/10.1007/s13399-020-00655-8>
- Pituya P, Sriburi T, Wijitkosum S (2017) Optimization of biochar preparation from acacia wood for soil amendment. *Eng J* 21:99–105. <https://doi.org/10.4186/ej.2017.21.2.99>
- Menya E, Olupot PW, Storz H, Lubwama M, Kiros Y, John MJ (2020) Optimization of pyrolysis conditions for char production from rice husks and its characterization as a precursor for production of activated carbon. *Biomass Conv Bioref* 10:57–72. <https://doi.org/10.1007/s13399-019-00399-0>
- Januszkiwicz J, Sabik H, Azamia S, Lee B (2008) Optimization of headspace solid-phase microextraction for the analysis of specific flavors in enzyme modified and natural Cheddar cheese using factorial design and response surface methodology. *J Chromatogr A* 1195:16–24. <https://doi.org/10.1016/j.chroma.2008.04.067>
- Siddiqui MTH, Nizamuddin S, Mubarak NM, Shirin K, Aijaz M, Hussain M, Baloch HA (2019) Characterization and process optimization of biochar produced using novel biomass, waste pomegranate peel: a response surface methodology approach. *Waste Biomass Valor* 10:521–532. <https://doi.org/10.1007/s12649-017-0091-y>
- Mazac R (2016) Assessing the use of food waste biochar as a biodynamic plant fertilizer. Departmental Honors Projects. 43. College of Liberal Arts, Hamline University. <https://digitalcommons.hamline.edu/dhp/43>. Accessed Oct 2020
- Basak T, Lou Z, Rahman MRT, Azam MS (2014) Quality evaluation of dehydrated (sun and solar drying) cabbage and rehydration properties. *Eur Acad Res* 2:8214–8243
- ASTM (2007) Standard test method for particle-size analysis of soils D 422-63
- Dai Z, Meng J, Muhammad N, Liu X, Wang H, He Y, Brookes PC, Xu J (2013) The potential feasibility for soil improvement, based on the properties of biochars pyrolyzed from different feedstocks. *J Soils Sediments* 13:989–1000. <https://doi.org/10.1007/s11368-013-0698-y>

32. Singh B, Dolk MM, Shen Q, Camps-Arbestain M (2017) Biochar pH, electrical conductivity and liming potential. In: *Biochar: A Guide to Analytical Methods*. Csiro Publishing, Clayton, pp 23–38
33. ASTM (2010) Standard test method for measuring the exchange complex and cation exchange capacity of inorganic fine-grained soils D7503-10
34. Qi F, Yan Y, Lamb D, Naidu R, Bolan NS, Liu Y, Ok YS, Donne SW, Semple KT (2017) Thermal stability of biochar and its effects on cadmium sorption capacity. *Bioresour Technol* 246:48–56. <https://doi.org/10.1016/j.biortech.2017.07.033>
35. ASTM (2013) Standard test methods for proximate analysis of coal and coke by macro thermogravimetric analysis D 7582-15
36. Islam M, Halder M, Siddique MAB, Razir SAA, Sikder S, Joardar JC (2019) Banana peel biochar as alternative source of potassium for plant productivity and sustainable agriculture. *Int J Recycl Org Waste Agric* 8:407–413. <https://doi.org/10.1007/s40093-019-00313-8>
37. Burcu Uzun B, Apaydin-Varol E, Ates F et al (2010) Synthetic fuel production from tea waste: characterisation of bio-oil and bio-char. *Fuel* 89:176–184. <https://doi.org/10.1016/j.fuel.2009.08.040>
38. Jindo K, Mizumoto H, Sawada Y, Sanchez-Monedero MA, Sonoki T (2014) Physical and chemical characterization of biochars derived from different agricultural residues. *Biogeosciences* 11: 6613–6621. <https://doi.org/10.5194/bg-11-6613-2014>
39. Junna S, He F, Shao H et al (2016) Effects of biochar application on Suaeda salsa growth and saline soil properties. *Environ Earth Sci* 75:630. <https://doi.org/10.1007/s12665-016-5440-9>
40. Xue S, Zhang X, Ngo HH, Guo W, Wen H, Li C, Zhang Y, Ma C (2019) Food waste based biochars for ammonia nitrogen removal from aqueous solutions. *Bioresour Technol* 292:121927. <https://doi.org/10.1016/j.biortech.2019.121927>
41. Matsumoto S, Ogata S, Shimada H, Sasaoka T, Hamanaka A, Kusuma G (2018) Effects of pH-induced changes in soil physical characteristics on the development of soil water erosion. *Geosciences* 8:134
42. Tomczyk A, Sokołowska Z, Boguta P (2020) Biochar physico-chemical properties: pyrolysis temperature and feedstock kind effects. *Rev Environ Sci Biotechnol* 19:191–215. <https://doi.org/10.1007/s11157-020-09523-3>
43. Machado R, Serralheiro R (2017) Soil salinity: effect on vegetable crop growth. Management practices to prevent and mitigate soil salinization. *Horticulturae* 3:–13. <https://doi.org/10.3390/horticulturae3020030>
44. Domingues RR, Trugilho PF, Silva CA, Melo ICNA, Melo LCA, Magriotis ZM, Sánchez-Monedero MA (2017) Properties of biochar derived from wood and high-nutrient biomasses with the aim of agronomic and environmental benefits. *PLoS One* 12:e0176884. <https://doi.org/10.1371/journal.pone.0176884>
45. Piash MI, Hossain MF, Parveen Z (2016) Physico-chemical properties and nutrient content of some slow pyrolysis biochars produced from different feedstocks. *Bangladesh J Sci Res* 29:111–122. <https://doi.org/10.3329/bjsr.v29i2.32327>
46. Clough TJ, Condrón LM, Kammann C, Müller C (2010) Biochar and the nitrogen cycle: introduction. *J Environ Qual* 39:1218–1223. <https://doi.org/10.2134/jeq2010.0204>
47. Gao G, Falconer RA, Lin B (2015) Modelling the fate and transport of faecal bacteria in estuarine and coastal waters. *Mar Pollut Bull* 100:162–168. <https://doi.org/10.1016/j.marpolbul.2015.09.011>
48. Rawat J, Saxena J, Sanwal P (2019) Biochar: a sustainable approach for improving plant growth and soil properties. In *Biochar-an imperative amendment for soil and the environment. Fruit and vegetable waste: bioactive compounds, their extraction, and possible utilization*. DOI: <https://doi.org/10.5772/intechopen.82151>
49. Budai A, Zimmerman AR, Cowie AL, et al (2013) Biochar carbon stability test method: an assessment of methods to determine biochar carbon stability. *Int Biochar Initiat* 1–10
50. Billa SF, Angwafo TE, Ngome AF (2019) Agro-environmental characterization of biochar issued from crop wastes in the humid forest zone of Cameroon. *Int J Recycl Org Waste Agric* 8:1–13. <https://doi.org/10.1007/s40093-018-0223-9>
51. Stella Mary G, Sugumaran P, Niveditha S, Ramalakshmi B, Ravichandran P, Seshadri S (2016) Production, characterization and evaluation of biochar from pod (*Pisum sativum*), leaf (*Brassica oleracea*) and peel (*Citrus sinensis*) wastes. *Int J Recycl Org Waste Agric* 5:43–53. <https://doi.org/10.1007/s40093-016-0116-8>

**Publisher's note** Springer Nature remains neutral with regard to jurisdictional claims in published maps and institutional affiliations.